FDG PET/MR in initial staging of sarcoma: Initial experience and comparison with conventional imaging

Platzek, I.; Beuthien-Baumann, B.; Schramm, G.; Maus, J.; Laniado, M.; Kotzerke, J.; van den Hoff, J.; Schuler, M.;

Originally published:

November 2016

Clinical Imaging 42(2017), 126-132

DOI: https://doi.org/10.1016/j.clinimag.2016.11.016

FDG PET/MR in initial staging of sarcoma: Initial experience and comparison with conventional imaging

Ivan Platzek, Bettina Beuthien-Baumann, Georg Schramm, Jens Maus, Michael Laniado, Jörg Kotzerke, Jörg van den Hoff, Markus Schuler

PII: S0899-7071(16)30189-9
DOI: doi:10.1016/j.clinimag.2016.11.016
Reference: JCT 8157

To appear in: *Journal of Clinical Imaging*

Received date: 18 July 2016
Revised date: 10 November 2016
Accepted date: 28 November 2016

Please cite this article as: Platzek Ivan, Beuthien-Baumann Bettina, Schramm Georg, Maus Jens, Laniado Michael, Kotzerke Jörg, van den Hoff Jörg, Schuler Markus, FDG PET/MR in initial staging of sarcoma: Initial experience and comparison with conventional imaging, *Journal of Clinical Imaging* (2016), doi:10.1016/j.clinimag.2016.11.016

Manuscript title:

FDG PET/MR in initial staging of sarcoma: initial experience and comparison with conventional imaging

Authors:
Ivan Platzek, MD (corresponding author)
Dresden University Hospital, Department of Radiology,
Fetscherstr. 74, 01307 Dresden, Germany
phone: +49 351 458 18223
fax: +49 351 458 5758
Email: ivan.platzek@uniklinikum-dresden.de

Bettina Beuthien-Baumann, MD
Dresden University Hospital, Department of Nuclear Medicine,
Fetscherstr. 74, 01307 Dresden, Germany

Georg Schramm, PhD
Helmholtz-Zentrum Dresden-Rossendorf, Institute of Radiopharmaceutical Cancer Research,
Bautzner Landstr. 400, 01328 Dresden, Germany

Jens Maus, PhD
Helmholtz-Zentrum Dresden-Rossendorf, Institute of Radiopharmaceutical Cancer Research,
Bautzner Landstr. 400, 01328 Dresden, Germany

Michael Laniado, MD
Dresden University Hospital, Department of Radiology,
Fetscherstr. 74, 01307 Dresden, Germany

Jörg Kotzerke, MD
Dresden University Hospital, Department of Nuclear Medicine,
Fetscherstr. 74, 01307 Dresden, Germany

Jörg van den Hoff, PhD
Helmholtz-Zentrum Dresden-Rossendorf, Institute of Radiopharmaceutical Cancer Research,
Bautzner Landstr. 400, 01328 Dresden, Germany

Markus Schuler, MD
Dresden University Hospital, Department of Internal Medicine
Fetscherstr. 74, 01307 Dresden, Germany

Manuscript title:

FDG PET/MR in initial staging of sarcoma: initial experience and comparison with conventional imaging

Abstract

Objective:

To assess the feasibility of positron emission tomography/magnetic resonance imaging (PET/MR) with 18F-fluordeoxyglucose (FDG) for initial staging of sarcoma.

Materials and methods:

Twenty-nine patients with sarcoma were included in this study. Weighted kappa (κ) was used to assess the agreement between PET/MR and conventional imaging (CT and MR). The accuracy of PET/MR and conventional imaging for distant metastases was compared using receiver operating characteristic (ROC) analysis.

Results:

T and M stage were identical for PET/MR and conventional modalities in all patients ($\kappa = 1$). N stage was identical for 28/29 patients ($\kappa = 0.65$).

Conclusions:

FDG PET/MR shows excellent agreement with the currently preferred imaging methods (CT and MR) in initial staging of sarcoma.

Keywords:

Sarcoma, PET/MR, staging

Introduction

Sarcomas are a heterogeneous group of tumors, which make up about 1% of all malignancies in adults [1, 2]. Beside sarcoma type, important factors for the choice of therapy and prognosis in sarcoma include the extent of the primary tumor and the presence of metastases. Initial staging in sarcoma currently relies mostly on MR (magnetic resonance imaging) for primary tumor assessment and CT (computed tomography) for evaluation of possible distant metastases [3]. While whole-body MR has been feasible for nearly a decade, it has not been evaluated in sarcoma patients. The recently introduced hybrid imaging modality PET/MR (positron emission tomography /magnetic resonance imaging) combines the excellent soft tissue contrast of MR and metabolic information provided by PET. When compared to standalone imaging modalities or PET/CT, the combination of PET and MR is expected to improve metastasis detection, for example in regard to cerebral, hepatic or musculoskeletal metastases[4], partly due to the superior soft tissue contrast of MR . Besides morphologic imaging with excellent contrast, PET/MR also allows for diffusion-weighted imaging (DWI) or imaging with supraparamagnetic nanoparticles, which can provide additional information about tissue properties and can also be advantageous for metastasis detection. Thus PET/MR provides an interesting new alternative in tumor imaging. Potential advantages of FDG PET/MR have already been

demonstrated in patients with head and neck cancer[5], lung cancer [6] and breast cancer [7]. The use of PET/MR in sarcoma staging has not been systematically evaluated yet. The aim of this study was to assess the feasibility of PET/MR with FDG (18F-fluordeoxyglucose) in initial staging of sarcoma and evaluate the agreement of PET/MR and conventional imaging modalities (computed tomography = CT; and MR) regarding sarcoma staging. The study also compared the sensitivity and specificity of PET/MR and conventional imaging modalities for distant metastases.

Materials and methods

This retrospective study was approved by the local ethics committee and written informed consent was waived.

The radiology information system (RIS) of our hospital was searched for patients who underwent FDG PET/MR for initial staging of sarcoma between January 2011 and December 2014. Besides whole-body FDG PET/MR, a dedicated MR of the primary tumor and a contrast-enhanced CT of the thorax and abdomen for initial staging were also inclusion criteria.

Twenty-nine consecutive patients with histologically confirmed sarcoma fulfilled the requirements mentioned above and were included in the study (13 f, 16 m, mean age 52 y, age range 18 – 77 y). In these patients, FDG PET/MR, MR of the primary tumor, and contrast-enhanced CT were performed within a time interval 16 days or less.

Sarcoma types included pleomorphic sarcoma (n =11), myxoid liposarcoma (n = 3), myxofibrosarcoma (n = 3), rhabdomyosarcoma (n = 2), leiomyosarcoma (n = 2), osteosarcoma (n = 2), epitheloid sarcoma (n = 1), Ewing sarcoma (n = 1), alveolar soft part sarcoma (n = 1), synovial sarcoma (n = 1), high-grade liposarcoma (n = 1) and myxoid chondrosarcoma (n = 1). Primary tumor locations included the extremities (n = 22), the thoracic wall (n =3), the lung (n = 1), retroperitoneum (n = 1), peritoneum (n = 1), and mediastinum (n = 1).

Information on therapy was available in 28/29 patients (96.5%). Therapy consisted of:

- Amputation of the affected extremity, preceded by neoadjuvant chemotherapy in 3/28 patients (10.7%)
- Tumor resection, preceded by neoadjuvant chemotherapy in 6/28 patients (21.4%)
- Tumor resection, preceded by neoadjuvant chemotherapy, and followed by pulmonary metastasis resection in 1/28 patients (3.6%)

- Tumor resection, preceded by neoadjuvant chemotherapy and followed by adjuvant chemotherapy in 1/28 patients (3.6%)
- Tumor resection, preceded by neoadjuvant chemotherapy and followed by adjuvant radiotherapy in 4/28 patients (14.3%)
- Tumor resection, followed by adjuvant radiotherapy in 6/28 patients (21.4%)
- Palliative chemotherapy in 6/28 patients (21.4%)
- Neoadjuvant radiotherapy, followed by symptomatic palliative radiotherapy of a vertebral metastasis in 1/28 patients (3.6%)

One patient was not treated at our hospital and no information about later treatment received at other institutions was available.

Six patients were not included as they had FDG PET/MR, MR of the primary tumor and chest CT, but no abdominal CT.

The standard of reference in regard to metastatic lesions was based on a consensus reading follow-up imaging examinations and on histology findings. Based on the standard of reference the lesions were classified as either benign of malignant. Histological correlation for lesions other than the primary tumor was available only in three patients (pulmonary metastases in all three cases).

Follow-up imaging was available in all patients and included contrast-enhanced computed tomography CT and MR in all cases, and also PET/MR in three patients The time interval between FDG PET/MR and the latest follow-up imaging available was 28 months on average (between 6 and 55 months). The consensus reading of follow-up imaging was undertaken together by two radiologists (11 years experience with CT and MR; 7 years experience with CT and 5 years experience with MR, respectively). As the radiologists were already involved in the valuation of PET/MR or the conventional modalities, the reading of the follow-up imaging was undertaken four months after those reading to avoid bias.

FDG PET/MR

18F-fluordeoxyglucose (FDG) was used as a radiotrace in the PET/MR examinations. The patients were instructed to fast for at least six hours prior to the FDG injection. All patients were injected intravenously with 4.5 MBq FDG/ kg body weight (252-331 MBq FDG, 297.7 MBq average). The average time between the tracer injection and the start of the PET scan was 71 min (53-112 min). Blood glucose level at the time of the tracer injection varied between 4.3 and 12.1 mmol/l (5.8 mmol/l on average).

PET/MR was performed on a hybrid PET/MR system (Philips Ingenuity TF PET/MR, Best, The Netherlands) equipped with a 3T main magnet. The system `s integrated body coil was used for signal acquisition. The examination was performed with the patient in the supine position. The position of the patient on the scanner table remains unchanged during the whole exam in order to achieve optimal spatial correlation of PET and MR. The PET/MR exam consisted of an ``attenuation MR" (atMR) whole-body scan, followed by a PET scan and diagnostic MR. A multistation technique is used to achieve sufficient coverage for both PET and MR.

atMR is a T1-weighted gradient echo scan used for PET attenuation correction, and is performed in free breathing. atMR was performed with 4.1 ms/2.3 ms (repetition time/echo time), a field of view of 600 x 600 mm, and a slice thickness of 6 mm. Twelve contiguous sets of atMR images (= stacks) are needed to achieve adequate coverage. Stack thickness was 120 mm. Total acquisition time for the atMR is 03:18 min.

The extent of the PET scan varied depending on tumor location. In 24 patients, the PET scan covered the whole body (overlapping scans at 21 or 22 contiguous bed positions), while in five patients the PET scan covered the head, neck, thorax, abdomen and pelvis, but not the lower extremities (11 contiguous bed positions). Acquisition time was 2 min for each of the eleven bed positions covering the head, neck, thorax, abdomen and pelvis and 1:30 min for each of

the bed positions covering the lower extremities (max. 37.5 min in total for whole body coverage and 22 min in patients without coverage of the lower extremities). Attenuation correction of the PET dataset was based on the previously mentioned atMR, applying segmentation and tissue type identification [8].

Diagnostic MR included whole body THRIVE (T1 high resolution isotropic volume excitation) scans with and without contrast enhancement and STIR (short tau inversion recovery) images of the primary tumor. Both contrast-enhanced and nonenhanced THRIVE images were acquired with fat suppression).

The whole-body THRIVE MR scan consists of nine contiguous bed positions (i.e. stacks), with combined acquisition time of 2:50 min. THRIVE image stacks were acquired with 2.2 ms/4.5 ms (repetition time/echo time), a slice thickness of 4 mm, a stack thickness of 200 mm, a field-of-view of 450 x 322 mm and an acquisition time of 19 s. For the stacks covering the thorax, abdomen and pelvis, the signal was acquired in breath hold, while the remaining body regions (head/neck and lower extremities) are examined in free breathing.

Before the acquisition of contrast-enhanced THRIVE images, 0.2 ml/body weight Gd DTPA (Magnevist®, Bayer Healthcare, Berlin, Germany) was administered intravenously.

Short tau inversion recovery (STIR) images of the tumor region in transverse orientation were acquired with 4657 ms/217 ms/ 220 ms (repetition time/echo time/inversion time), a slice thickness of 6 mm, a matrix of 512 x 512 and an acquisition time of 5:30 min.

Total imaging time for the PET/MR exam was 37 – 52.5 min, including 22 – 37.5 min PET scan time.

CT

All patients underwent contrast-enhanced CT of the thorax and abdomen. CT scans were performed on a 128-slice CT system (Somatom AS+, Siemens Medical Solutions, Erlangen, Germany). The examination was performed with a single collimation width of 0.75 mm, a table feed speed of 30.7 mm per rotation, and a pitch of 0.8.

The patients were injected with 80 ml Iopromide 370 (Ultravist 370, Bayer Pharma AG, Berlin, Germany). The contrast agent was administered in an antecubital vein using a 18 gauge intravenous catheter and with a flow rate of 3 ml/s. Contrast injection was followed by a 50 ml saline flush with a flow rate of 3 ml/s. A dual syringe CT injection system (Stellant, Medrad, Indianola, PA, USA) was used for injection of both the contrast medium and the saline flush.

The CT examination included an arterial phase scan of the thorax and upper abdomen, with 30 s contrast delay time, and an venous phase scan of the

abdomen and pelvis, with 70 s contrast delay time. Axial CT images were reconstructed with 1 mm and 3 mm slice thickness.

MR

Standalone MR of the tumor region was performed on a 3T MR system (Verio, Siemens Medical Solutions, Erlangen, Germany). The choice of field-of-view varied depending on the tumor location. A 6-channel body coil was used for signal acquisition. The standalone MR examination included T1-weighted turbo spin echo (TSE) images with and without fat saturation, and TIRM (tau inversion recovery magnitude) TSE images. T1 –weighted TSE images in transverse orientation were acquired with 782 ms/11 ms (repetition time/echo time), a slice thickness of 4 mm and a matrix of 512 x 512. TIRM TSE images in transverse orientation were acquired with 5892 ms/79 ms/170 ms (repetition time/echo time/inversion time), a slice thickness of 4 mm, and a matrix of 384 x 384. TIRM images in coronal orientation were acquired with 7821 ms/74 ms/170 ms (repetition time/echo time/inversion time), a slice thickness of 4 mm and a matrix of 384 x 384.

Before the acquisition of contrast-enhanced MR images, the patients received an intravenous injection of 0.2 ml/body weight Gd DTPA (Magnevist®, Bayer Healthcare, Berlin, Germany), followed by 20 ml saline flush.

T1-weighted contrast-enhanced (CE) TSE images with fat saturation were acquired with 581 ms/ 11 ms (echo time/repetition time), a slice thickness 4 mm, and a matrix of 384 x 384.

T1-weighted CE TSE images with fat saturation in coronal orientation were also acquired with 581 ms/11 ms (repetition time/echo time), a slice thickness of 4 mm and a matrix of 384 x 384.

Depending on tumor size, MR acqusition time was 24 – 29 min.

Image evaluation

PET/MR examinations were evaluated together by a board-certified nuclear medicine physician with 20 years experience with PET and a board-certified radiologist with 11 years of experience with MR. The readers were blinded for all other imaging. In addition, both readers were blinded in regard to sarcoma type. Lesions which appeared to have increased FDG uptake in comparison to the surrounding structures were considered malignant [9, 10]. The ROVER® software package (ABX advanced biochemical compounds, Radeberg, Germany) was used for PET viewing and evaluation. [11]. On MR images, irregular lesion borders and necrosis were considered signs of malignancy [12]. Increased lymph node size was considered a sign of malignancy, with size thresholds depending on location [13-15]. Lymph node necrosis and contour

irregularities were also considered a sign of metastatic disease. Tumor size measurements were based on the transverse contrast-enhanced THRIVE MR images. The TNM staging system [16] was used to describe disease stage, based on the consensus findings of the radiologist and the nuclear medicine physician.

Conventional imaging modalities (CT and MR) were evaluated by a board-certified radiologist with 7 years of experience in CT and 5 years of experience in MR. This radiologist was blinded to PET/MR images. Malignancy criteria were identical to those described above for MR images. The radiologist responsible for the reading of the CT and MR examinations also summarized his findings according to the TNM classification.

In addition, lesions other than primary tumors and suspected locoregional metastases were rated according to a five-point scale: 0 = benign, 1 = probably benign, 2 = equivocal, 3 = probably malignant, 4 = malignant.

Statistical analysis

Weighted kappa (κ) was used[17] to assess the agreement between PET/MR and conventional imaging modalities (CT and MR) in regard to T, N and M stage. κ-values were interpreted according to thresholds proposed by Landis and Koch (with $\kappa \leq 0$ being poor agreement, 0.01−0.2, slight agreement, 0.21−0.4, fair

agreement; 0.41−0.6, moderate agreement; 0.61−0.8, substantial agreement; and 0.81−1, almost perfect agreement)[18].

Receiver operating characteristic (ROC) analysis was used to compare FDG PET/MR and CT + MR in regard to accuracy for distant metastases. ROC curves were generated for the likelihood of malignancy in each lesion. Sensitivity and specificity were also calculated, with equivocal cases considered positive.

Data were analyzed using MedCalc 12.0 (MedCalc Software, Ostend, Belgium).

Results

The primary tumor was identified on PET/MR and MR in all patients (100% detection rate).

Twenty-seven of 29 primary tumors had increased FDG uptake in comparison to the surrounding tissues (SUV_{max} 4.2-23.6, mean SUV_{max} 12.3). Two patients with myxoid liposarcoma had minimally increased FDG uptake (SUV_{max} 2.3 and 2.9, respectively).

Based on the morphologic information of the PET/MR findings, the following T stages were assigned: T1b (n = 3), T2a (n = 3), T2b (n = 23). Based on metabolic and morphologic information of PET/MR N stage was found to be N0

in 27/29 patients and N1 in 2/29 patients. Based on PET/MR findings, the following stage M stage was assigned: M0 (n = 19), M1 (n = 10).

Based on CT and MR, the patients were assigned the following T stages: T1b (n = 3), T2a (n = 3), T2b (n = 23). In addition, the combined reading of CT and MR resulted in the following N stages: N0 (n = 28) and N1 (n = 1). The combination of CT and MR detected a distant metastasis in 10 patients (M1), while in the remaining 19 patients no distant metastases were detected (M0).

TNM results are summarized in Table 1.T and M stage was identical for PET/MR and the conventional modalities in all 29 patients ($\kappa = 1$). The case of a patient with identical TNM findings on both PET/MR and conventional modalities is demonstrated on Fig 1 and Fig 2. N stage differed between the methods in one patient (Fig 3 and 4) and was identical for the remaining 28 patients ($\kappa = 0.65$). The patient with differing N stages had a rhabdomyosarcoma of the thoracic wall and was classified as N1 based on PET/MR (due to increased FDG uptake in a normal-sized axillary lymph node), but as N0 based on CT (as there were no enlarged locoregional lymph nodes).

Retrospective evaluation showed no evidence of therapy change effected by the additional information provided by FDG PET/MR, when compared to the conventional imaging (MR and CT). As mentioned above, the only difference between FDG PET/MR and the conventional modalities was in regard to N stage

in a patient with a rhabdomyosarcoma of the thoracic wall. In this case, the axillary lymph node metastasis suspected on PET/MR did not lead to a change in the therapy regimen (adjuvant radiochemotherapy, followed by forequarter amputation.

The low number of suspected lymph node metastases does not suffice for a meaningful evaluation of the accuracy of the respective imaging methods in this regard.

As mentioned above, the lesion-based accuracy of the imaging methods in regard to distant metastases was evaluated using imaging follow-up as the standard of reference. In case of multiple metastases, ten metastases were included in the evaluation for each organ involved. Multiple metastases were present in four patients. Based on the consensus reading of the reference standard, 112 lesions were identified in total, 90 metastases and 22 benign lesions.

Lesion scores were identical for FDG PET/MR and conventional imaging in 98/112 (87.5%) lesions and differed in 14/112 lesions (12.5%). The distribution of lesion scores for each modality is summarized in Table 3. ROC analysis showed the sensitivity of FDG/PET MR for distant metastases to be 97.8% and the specificity 100%. Conventional imaging had a sensitivity of 94.4% and specificity of 100%, respectively. In addition, ROC analysis (Fig. 5) showed no

significant difference between the accuracy of FDG PET/MR and conventional imaging ($p = 0.51$).

Discussion

To our knowledge, the current study is the first to systematically evaluate the role of PET/MR in initial staging of sarcoma. A previous pilot study has already demonstrated the promise of FDG PET/MR in therapy response assessment in sarcoma[19]. However, in regard to initial staging of sarcoma, the use of PET/MR has only been mentioned in case reports[20]. Our study was able to show that FDG PET/MR is feasible for sarcoma staging and is comparable to the currently predominant combination of MR and CT in regard to sarcoma staging. Furthermore, there was no evidence of therapy change caused by the additional information provided by FDG PET/MR. Our results are comparable to the earlier studies which investigated the role of PET/CT and standalone PET in sarcoma staging. For example, Tateishi et al. found no significant difference between FDG PET/CT and conventional imaging (in this case a combination of MR, CT, chest X-ray and bone scintigraphy) in regard to TNM staging in sarcoma [21]. Iagaru et al. [22] found that while FDG PET/CT has a high sensitivity and specificity in initial staging of sarcoma, it did not improve the sensitivity and specificity of CT.

In regard to distant metastases, our study differs from Völker et. al., who found that FDG PET was equal to conventional imaging modalities (ultrasound, CT, MR and bone scintigraphy) for primary tumor detection in pediatric sarcoma patients, while it was superior for detection of bone metastases [23]. In our study, bone metastases detected by FDG PET/MR were also detected by CT. However, only two patients in our study had bone metastases. Thus additional data are needed to allow for a meaningful evaluation of the impact of FDG PET/MR on bone metastasis detection.

While the current pilot study does not imply an advantage of PET/MR over conventional imaging for initial staging of sarcoma, the combined information provided by PET/MR may nevertheless be useful for several reasons. One benefit of FDG PET/MR in sarcoma over standalone MR is the prognostic value of PET. For example, Hong et al. were able to show that SUV_{max} of the primary tumor in FDG PET/CT is an important prognostic factor for overall survival in patients with soft tissue sarcoma [24]. Skamene et al. have also shown that SUV_{max} of the tumor is an negative prognostic factor in extremity sarcoma for both progression free survival and overall survival [25].

FDG PET/MR is also promising because of its potentially improved ability for monitoring therapy response in comparison to standalone MR. A number of studies have demonstrated the utility of FDG PET for chemotherapy response assessment in soft tissue sarcoma. For example, Benz et al. [26] investigated the

use of FDG PET/CT in patients with soft tissue sarcoma receiving their first cycle of chemotherapy and demonstrated that a 35% reduction of FDG uptake is a sensitive predictor for therapy response. Similarly, Evilevitch et al. [27] were able to show that FDG uptake is better suited for evaluation of treatment response in soft tissue sarcoma than size criteria. While a detailed evaluation of FDG PET/MR in therapy response assessment in sarcoma is not yet available, a pilot study has already demonstrated that FDG PET/MR may provide useful additional information, as the disagreement between the new modality and MR on response assessment is rather substantial[19].

Future potential indication of FDG PET/MR in musculoskeletal imaging are not limited to malignant disease. The new hybrid modality may be helpful in inflammatory and infections diseases of the musculoskeletal system as well[28].

The main limitation of the current study is the heterogeneous patient cohort. Furthermore, the low number of patients with suspected nodal metastases (n = 2) may artificially lead to a lower method agreement on N staging as compared to T and M staging. Another shortcoming is the lack of histological correlation for suspected metastatic lesions. In addition, the study does not provide a comparison between PET/MR and the more widely available PET/CT. The lack of diffusion-weighted sequences in the PET/MR protocol is a further limitation, as such sequences could provide important additional information about the

tumor and possible metastases. The decision not to include diffusion-weighted sequences was mainly caused by time constraints.

In the current study, the scanner`s integrated body coil was used for signal acquisition, which typically leads to reduced image quality in comparison to surface coils [29] and may cause some lesions to be missed. The decision to use the integrated body coil for whole-body imaging is dictated by the scanner design, which only allows two surface coils to be used together without patient repositioning.

Conclusion

FDG PET/MR is feasible for initial staging of sarcoma and has high sensitivity and specificity for distant metastases. While our initial results show a very good agreement with conventional imaging modalities (CT and MR), the benefit of the addition of PET to whole body MR is not clear at this stage. Further evaluation is also needed to clarify a possible role of FDG PET/MR for therapy choice and therapy monitoring in sarcoma.

Reference

[1] Burningham Z, Hashibe M, Spector L, Schiffman JD. The epidemiology of sarcoma. Clin Sarcoma Res 2012;2(1):14.

[2] Gatta G, van der Zwan JM, Casali PG, Siesling S, Dei Tos AP, Kunkler I, et al. Rare cancers are not so rare: the rare cancer burden in Europe. Eur J Cancer 2011;47(17):2493-511.

[3] Mendenhall WM, Indelicato DJ, Scarborough MT, Zlotecki RA, Gibbs CP, Mendenhall NP, et al. The management of adult soft tissue sarcomas. Am J Clin Oncol 2009;32(4):436-42.

[4] Buchbender C, Heusner TA, Lauenstein TC, Bockisch A, Antoch G. Oncologic PET/MRI, part 2: bone tumors, soft-tissue tumors, melanoma, and lymphoma. J Nucl Med 2012;53(8):1244-52.

[5] Platzek I, Beuthien-Baumann B, Schneider M, Gudziol V, Kitzler HH, Maus J, et al. FDG PET/MR for lymph node staging in head and neck cancer. Eur J Radiol 2014;83(7):1163-8.

[6] Heusch P, Buchbender C, Kohler J, Nensa F, Gauler T, Gomez B, et al. Thoracic staging in lung cancer: prospective comparison of 18F-FDG PET/MR imaging and 18F-FDG PET/CT. J Nucl Med 2014;55(3):373-8.

[7] Pace L, Nicolai E, Luongo A, Aiello M, Catalano OA, Soricelli A, et al. Comparison of whole-body PET/CT and PET/MRI in breast cancer

patients: lesion detection and quantitation of 18F-deoxyglucose uptake in lesions and in normal organ tissues. Eur J Radiol 2014;83(2):289-96.

[8] Schramm G, Langner J, Hofheinz F, Petr J, Beuthien-Baumann B, Platzek I, et al. Quantitative accuracy of attenuation correction in the Philips Ingenuity TF whole-body PET/MR system: a direct comparison with transmission-based attenuation correction. MAGMA 2013;26(1):115-26.

[9] Boellaard R, O'Doherty MJ, Weber WA, Mottaghy FM, Lonsdale MN, Stroobants SG, et al. FDG PET and PET/CT: EANM procedure guidelines for tumour PET imaging: version 1.0. Eur J Nucl Med Mol Imaging 2010;37(1):181-200.

[10] Shankar LK, Hoffman JM, Bacharach S, Graham MM, Karp J, Lammertsma AA, et al. Consensus recommendations for the use of 18F-FDG PET as an indicator of therapeutic response in patients in National Cancer Institute Trials. J Nucl Med 2006;47(6):1059-66.

[11] Torigian DA, Lopez RF, Alapati S, Bodapati G, Hofheinz F, van den Hoff J, et al. Feasibility and performance of novel software to quantify metabolically active volumes and 3D partial volume corrected SUV and metabolic volumetric products of spinal bone marrow metastases on 18F-FDG-PET/CT. Hell J Nucl Med 2011;14(1):8-14.

[12] De Schepper AM, De Beuckeleer L, Vandevenne J, Somville J. Magnetic resonance imaging of soft tissue tumors. Eur Radiol 2000;10(2):213-23.

[13] van den Brekel MW, Castelijns JA, Snow GB. The size of lymph nodes in the neck on sonograms as a radiologic criterion for metastasis: how reliable is it? AJNR Am J Neuroradiol 1998;19(4):695-700.

[14] Glazer GM, Gross BH, Quint LE, Francis IR, Bookstein FL, Orringer MB. Normal mediastinal lymph nodes: number and size according to American Thoracic Society mapping. AJR Am J Roentgenol 1985;144(2):261-5.

[15] Dorfman RE, Alpern MB, Gross BH, Sandler MA. Upper abdominal lymph nodes: criteria for normal size determined with CT. Radiology 1991;180(2):319-22.

[16] Wittekind C, Meyer H-J, International Union against Cancer. TNM Klassifikation maligner Tumoren. 7. Aufl., 3. korr. Nachdr. ed. Weinheim: Wiley-Blackwell; 2011.

[17] Watson PF, Petrie A. Method agreement analysis: A review of correct methodology. Theriogenology 2010;73(9):1167-79.

[18] Landis JR, Koch GG. The measurement of observer agreement for categorical data. Biometrics 1977;33(1):159-74.

[19] Schuler MK, Platzek I, Beuthien-Baumann B, Fenchel M, Ehninger G, van den Hoff J. (18)F-FDG PET/MRI for therapy response assessment in sarcoma: comparison of PET and MR imaging results. Clin Imaging 2015;39(5):866-70.

[20] Loft A, Jensen KE, Lofgren J, Daugaard S, Petersen MM. PET/MRI for Preoperative Planning in Patients with Soft Tissue Sarcoma: A Technical Report of Two Patients. Case Rep Med 2013;2013:791078.

[21] Tateishi U, Yamaguchi U, Seki K, Terauchi T, Arai Y, Kim EE. Bone and soft-tissue sarcoma: preoperative staging with fluorine 18 fluorodeoxyglucose PET/CT and conventional imaging. Radiology 2007;245(3):839-47.

[22] Iagaru A, Quon A, McDougall IR, Gambhir SS. F-18 FDG PET/CT evaluation of osseous and soft tissue sarcomas. Clin Nucl Med 2006;31(12):754-60.

[23] Volker T, Denecke T, Steffen I, Misch D, Schonberger S, Plotkin M, et al. Positron emission tomography for staging of pediatric sarcoma patients: results of a prospective multicenter trial. J Clin Oncol 2007;25(34):5435-41.

[24] Hong SP, Lee SE, Choi YL, Seo SW, Sung KS, Koo HH, et al. Prognostic value of 18F-FDG PET/CT in patients with soft tissue sarcoma:

comparisons between metabolic parameters. Skeletal Radiol 2014;43(5):641-8.

[25] Skamene SR, Rakheja R, Dalhstrom KR, Roberge D, Nahal A, Charest M, et al. Metabolic activity measured on PET/CT correlates with clinical outcomes in patients with limb and girdle sarcomas. J Surg Oncol 2014;109(5):410-4.

[26] Benz MR, Czernin J, Allen-Auerbach MS, Tap WD, Dry SM, Elashoff D, et al. FDG-PET/CT imaging predicts histopathologic treatment responses after the initial cycle of neoadjuvant chemotherapy in high-grade soft-tissue sarcomas. Clin Cancer Res 2009;15(8):2856-63.

[27] Evilevitch V, Weber WA, Tap WD, Allen-Auerbach M, Chow K, Nelson SD, et al. Reduction of glucose metabolic activity is more accurate than change in size at predicting histopathologic response to neoadjuvant therapy in high-grade soft-tissue sarcomas. Clin Cancer Res 2008;14(3):715-20.

[28] Andersen KF, Jensen KE, Loft A. PET/MR Imaging in Musculoskeletal Disorders. PET Clinics 2016;11(4):453-63.

[29] Goyen M, Quick HH, Debatin JF, Ladd ME, Barkhausen J, Herborn CU, et al. Whole-body three-dimensional MR angiography with a rolling table platform: initial clinical experience. Radiology 2002;224(1):270-7.

Tables

Table 1

					FDG PET/MR			CT + MR		
Patient Nr.	Age	Sex	Tumor location	Tumor type	T	N	M	T	N	M
Soft tissue sarcoma										
1	48	m	left upper leg	rhabdomyosarcoma	T2a	N0	M0	T2a	N0	M0
2	53	f	left upper leg	leiomyosarcoma	T2b	N0	M0	T2b	N0	M0
3	62	f	left axilla	pleomorphic sarcoma	T2b	N1	M1	T2b	N1	M1
4	21	m	right upper arm	epitheloid sarcoma	T2b	N0	M0	T2b	N0	M0
5	42	f	left upper leg	myxoid liposarcoma	T2a	N0	M0	T2a	N0	M0
6	67	f	right upper leg	pleomorphic sarcoma	T2b	N0	M0	T2b	N0	M0
7	18	m	right thoracic wall	rhabdomyosarcoma	T2b	N1	M0	T2b	N0	M0
8	61	m	right upper leg	pleomorphic sarcoma	T2b	N0	M0	T2b	N0	M0
9	59	m	right upper leg	pleomorphic sarcoma	T2b	N0	M0	T2b	N0	M0
11	57	m	right lower leg	myxofibrosarcoma	T2b	N0	M0	T2b	N0	M0
12	77	m	right gluteal region	pleomorphic sarcoma	T2b	N0	M0	T2b	N0	M0
13	47	m	left lower leg	myxoid liposarcoma	T2b	N0	M0	T2b	N0	M0
14	72	m	right upper leg	myxofibrosarcoma	T2b	N0	M0	T2b	N0	M0

15	69	f	right upper leg	pleomorphic sarcoma	T1b	N0	M0	T1b	N0	M0
16	54	f	left upper leg	pleomorphic sarcoma	T2b	N0	M0	T2b	N0	M0
17	66	m	left lung	pleomorphic sarcoma	T2b	N0	M1	T2b	N0	M1
18	47	m	retroperitoneum	Ewing sarcoma	T2b	N0	M1	T2b	N0	M1
19	50	f	left shoulder	leiomyosarcoma	T1b	N0	M1	T1b	N0	M1
20	25	m	thoracic wall	alveolar soft part sarcoma (ASPS)	T1b	N0	M1	T1b	N0	M1
21	73	m	right upper leg	pleomorphic sarcoma	T2b	N0	M1	T2b	N0	M1
22	69	f	peritoneum	pleomorphic sarcoma	T2b	N0	M0	T2b	N0	M0
23	47	f	right upper leg	myxoid liposarcoma	T2b	N0	M0	T2b	N0	M0
24	41	f	left lower leg	pleomorphic sarcoma	T2a	N0	M0	T2a	N0	M0
25	61	m	left thoracic wall	myxofibrosarcoma	T2b	N0	M1	T2b	N0	M1
26	32	f	left upper leg	synovial sarcoma	T2b	N0	M1	T2b	N0	M1
27	73	f	mediastinum	high-grade liposarcoma	T2b	N0	M1	T2b	N0	M1
Bone sarcoma										
10	63	m	right upper arm	osteosarcoma	T2b	N0	M0	T2b	N0	M0
28	34	m	right upper leg	myxoid chondrosarcoma	T2b	N0	M0	T2b	N0	M0
29	25	f	right upper leg	osteosarcoma	T2b	N0	M1	T2b	N0	M1

Summary of FDG PET/MR staging results, compared with the combined results of CT and MRI. Soft tissue sarcoma and bone sarcoma are listed separately.

Table 2

Patient Nr.	Age	Sex	Tumor location	Tumor type	Location of metastases	Number of metastases
3	62	f	left axilla	pleomorphic sarcoma	right lung	2
17	66	m	left lung	pleomorphic sarcoma	left pleura	1
					left adrenal gland	1
18	47	m	retroperitoneum	Ewing sarcoma	both lungs	multiple
					liver	3
19	50	f	left shoulder	leiomyosarcoma	upper mediastinum	1
					left lower lung lobe	1
					mesenterium	2
					left gluteus maximus muscle	1
20	25	m	thoracic wall	alveolar soft part sarcoma (ASPS)	bones	4
21	73	m	right upper leg	pleomorphic sarcoma	both lungs	multiple
					spleen	multiple
25	61	m	left thoracic wall	myxofibrosarcoma	both lungs	multiple
					liver	multiple
					bones	multiple
26	32	f	left upper leg	synovial sarcoma	both lungs	multiple
27	73	f	mediastinum	high-grade liposarcoma	left lung	3
29	25	f	right	osteosarcoma	left lung	1

			upper leg			

Overview of distant metastases, identified using the standard of reference (imaging follow-up).

Table 3

FDG PET/MR scores	Conventional imaging scores (CT + MR)				
	1	2	3	4	5
1	14	2	3	0	0
2	3	2	3	0	0
3	0	0	0	0	2
4	0	0	0	1	2
5	1	0	2	1	79

Method agreement in regard to distant metastases. The following scores were used: 0 = benign, 1 = probably benign, 2 = equivocal, 3 = probably malignant, 4 = malignant. Lesion scores were identical for FDG PET/MR and conventional imaging in 98/112 (87.5%) lesions and differed in 14/112 lesions (12.5%)

Figure captions sarcoma

Fig 1
Sixty-three-year-old male patient with osteosarcoma of the right humerus. FDG PET/MR. A: transverse fused PET/MR image; B: corresponding contrast-enhanced THRIVE (T1 high resolution isotropic value excitation) MR image; C: PET MIP (maximum intensity projection). The tumor (green arrow) is readily recognizable due to the high FDG uptake and the strong contrast enchancement of its extraosseous component. There was no evidence of metastatic disease.

Fig 2
Same patient as Fig 1. A: T1-weighted MR without contrast enhancement; B: transverse, T1-eighted MR with contrast enhancement and fat saturation; C: contrast-enhanced CT. In analogy to the MR component of PET/MR, the tumor (green arrow) is readily recognizable on standalone MR. On CT, the tumor shows extraosseous calcifications, but is less well detectable due to the lower soft tissue contrast of CT. CT and MR did not show any findings suggestive of metastatic disease.

Fig 3
Eighteen-year-old male patient with a rhabdomyosarcoma of the thoracic wall; images from the PET/MR examination. A and B: transverse contrast-enhanced THRIVE images with fat saturation; C and D: corresponding fused PET/MR images; E: PET MIP image. The tumor (green arrow) shows both a strong MR contrast enhancement (A and B) and a high FDG uptake (C – E). A solitary, normal sized lymph node in the right axilla (red arrow) was suspected of metastatic disease because of its high FDG uptake.

Fig 4
Same patient as Fig 3. A and B: transverse contrast- enhanced CT; C and D: corresponding transverse STIR (short tau inversion recovery) MR images. The tumor (green arrow) is readily recognizable on the MR images, but barely recognizable on CT images. The axillary lymph node (red arrow), which showed increased FDG uptake in the PET/MR examination (Fig 1) is not enlarged and was rated as benign based on CT and MR.

Fig 5
ROC curves generated for detection of distant metastases by FDG PET/MR and conventional imaging modalities (CT + MR). There was no significant difference between the AUCs (areas under the curve) representing the accuracy of the respective imaging methods.

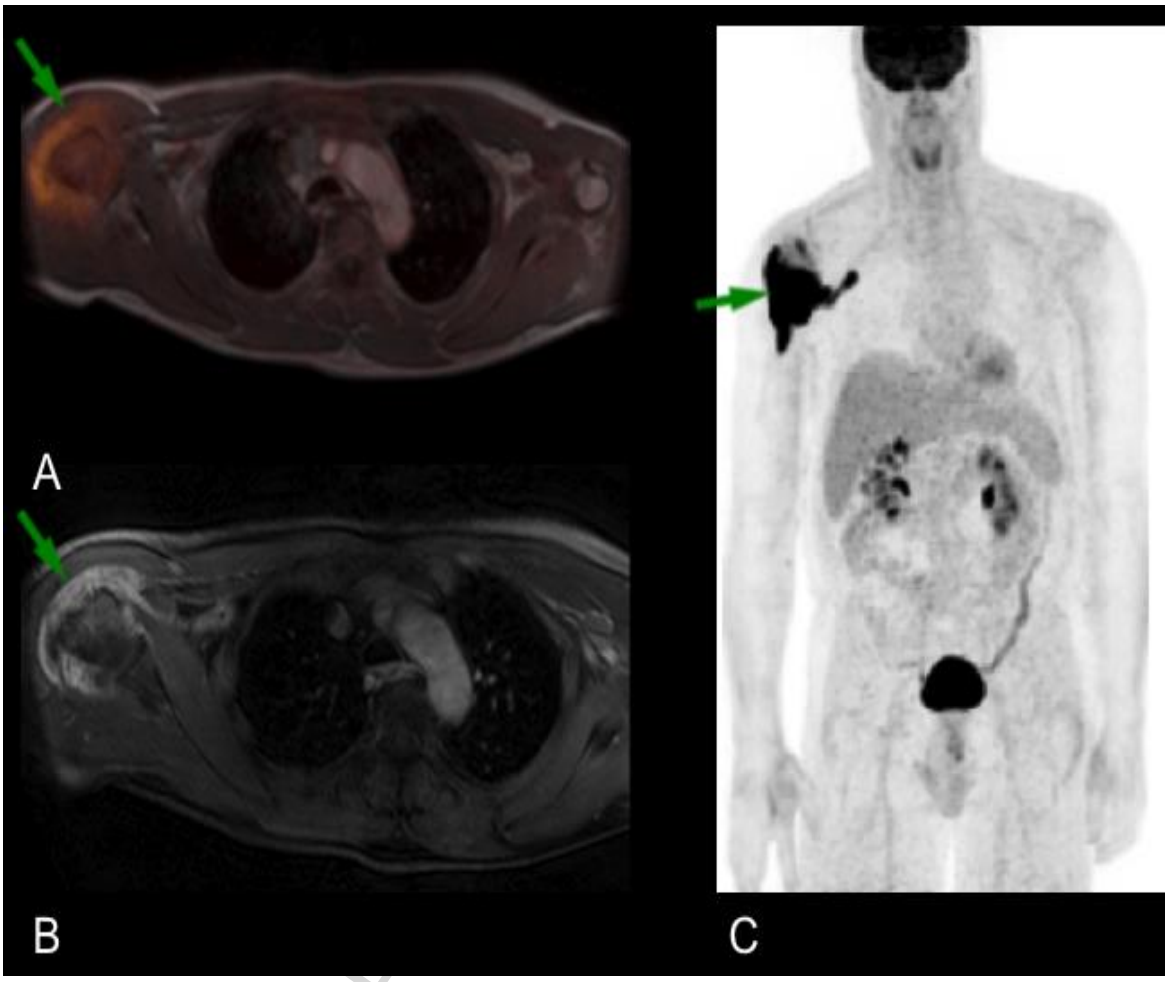

Fig. 1

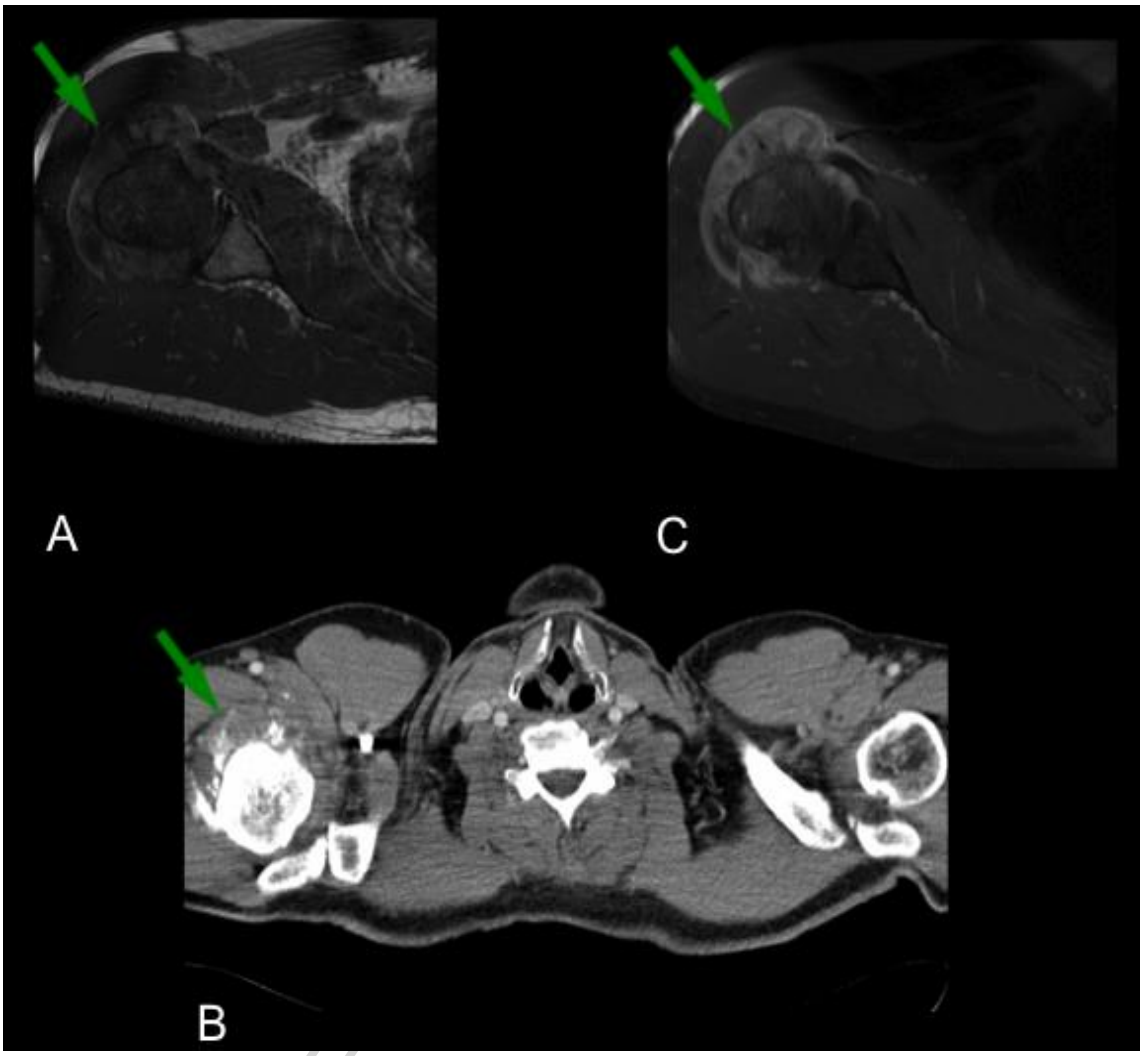

Fig. 2

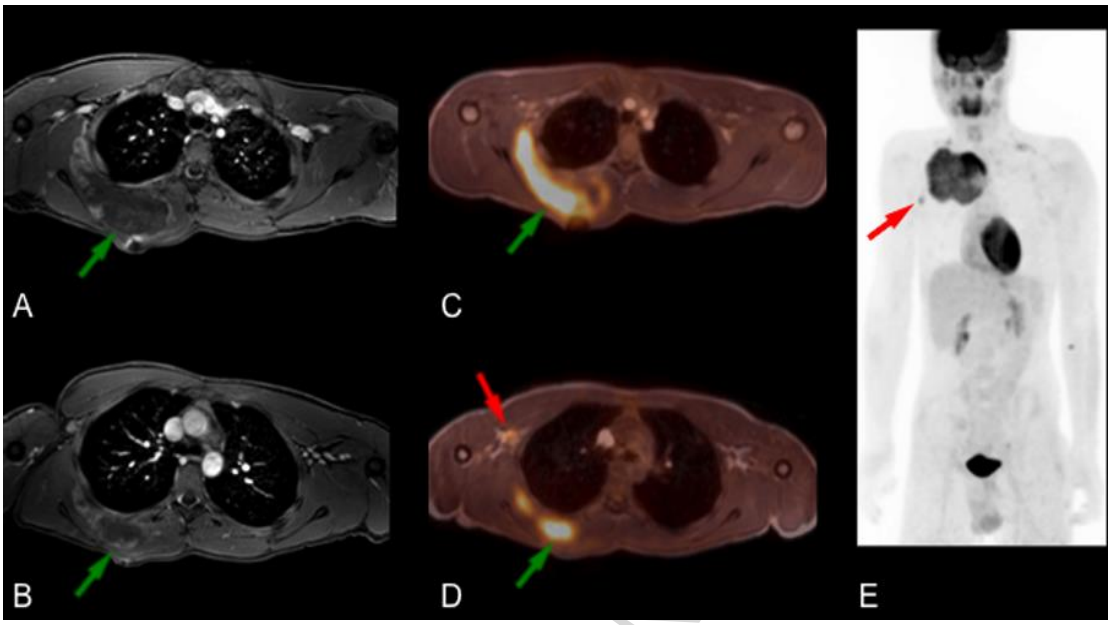

Fig. 3

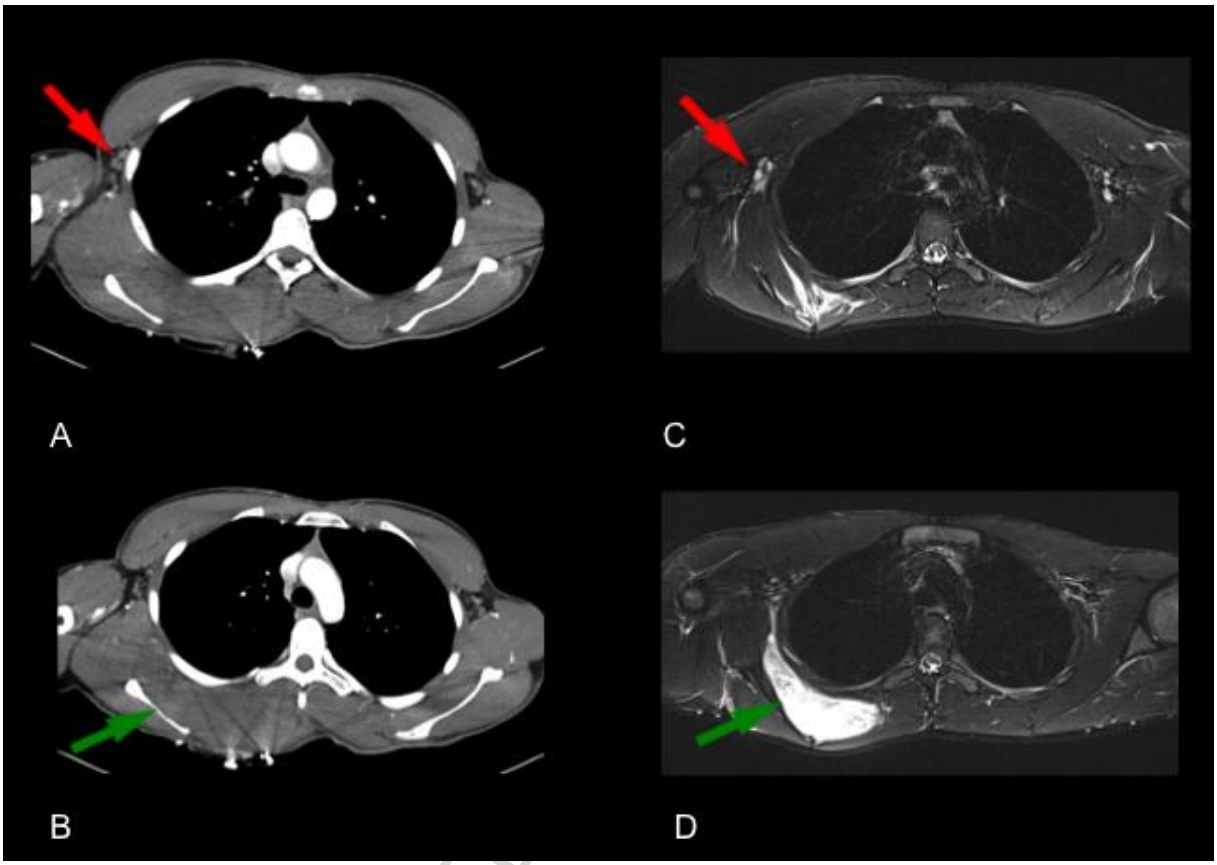

Fig. 4

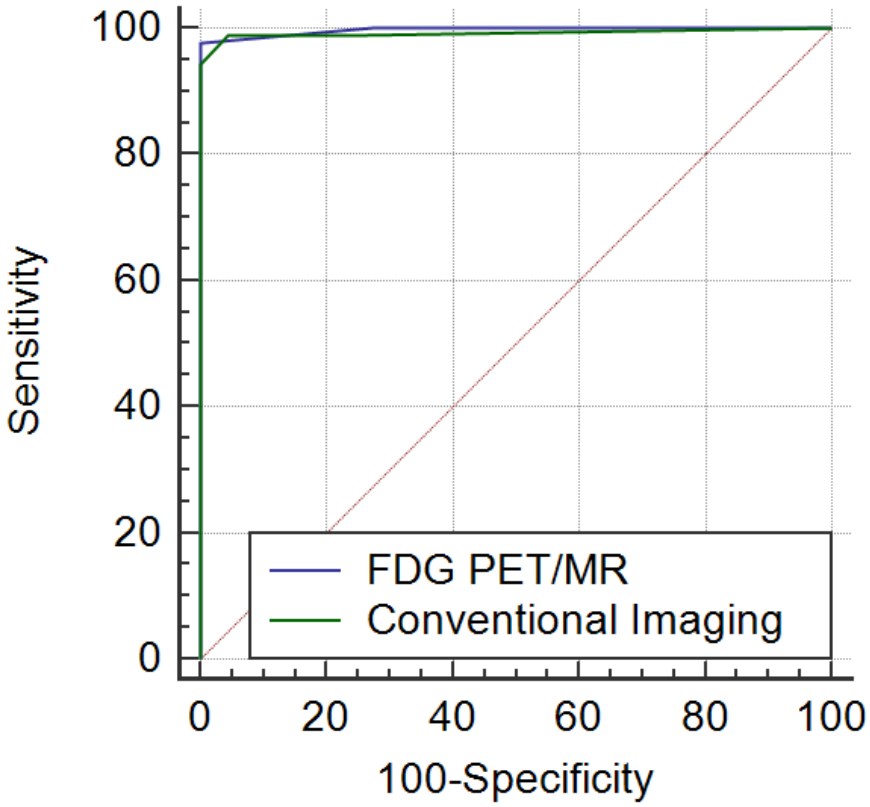

Fig. 5

Highlights

- T and M stage was identical for PET/MR and the conventional modalities (CT and MR) in all 29 patients (κ = 1)
- N stage differed between the methods in one patient and was identical for the remaining 28 patients (κ = 0.65)
- Our study shows that FDG PET/MR is feasible for initial staging of sarcoma and shows excellent agreement with the currently preferred imaging methods (a combination of CT and MR)